

NEW PREDICTIVE MODELS FOR THE BALLISTIC LIMIT OF SPACECRAFT SANDWICH PANELS SUBJECTED TO HYPERVELOCITY IMPACT

ALEKSANDR CHERNIAEV & RILEY CARRIERE

Department of Mechanical, Automotive and Materials Engineering, University of Windsor, Canada

ABSTRACT

Cell size, foil thickness, and the material of the core, influence the ballistic performance of honeycomb-core sandwich panels (HCSP) in the case of hypervelocity impact (HVI) by orbital debris. Two predictive models that account for this influence have been developed in this study: a dedicated ballistic limit equation (BLE) and an artificial neural network (ANN) trained to predict the outcomes of HVI on HCSP. The BLE is a modified version of the Whipple shield BLE and demonstrated excellent accuracy in predicting the ballistic limits of HCSP, when tested against a new set of simulation data, with the discrepancy ranging from 1.13% to 5.58% only. The ANN was developed using MATLAB's Deep Learning Toolbox framework and was trained utilizing the same HCSP HVI database as that employed for the BLE fitting and demonstrated a very good predictive accuracy, when tested against a set of simulation data not previously used in the training of the network, with the discrepancy ranging from 0.67% to 7.27%.

Keywords: orbital debris shielding, honeycomb-core sandwich panels, hypervelocity impact, ballistic limit equation, artificial neural network.

1 INTRODUCTION

For unmanned spacecraft, it is often possible to use pre-existing structural components as orbital debris shielding, thus designing multifunctional structures and enabling additional weight savings [1]. In a typical satellite design, most impact-sensitive equipment is situated in the enclosure of the structural honeycomb-core sandwich panels (HCSP). Being the most commonly used elements of satellite structures, these panels form the satellite's shape and are primarily designed to resist launch loads and provide attachment points for satellite subsystems [2]. With low additional weight penalties, their intrinsic ballistic performance can often be upgraded to the level required for orbital debris protection [3].

Assessing the orbital debris impact survivability of unmanned satellites requires reliable predictive models for honeycomb-core sandwich panels, capable of accounting for various impact conditions and panel design parameters. To make it applicable for HCSP and account for the presence of honeycomb core, Lathrop and Sennett [4] proposed modifying the well-known Whipple shield ballistic limit equation (eqn (1)) (normal incidence impact-only version):

$$D_{cr} = 3.918 \cdot \sqrt[3]{\frac{\bar{S}}{\rho_p \sqrt[3]{\rho_b}}} \cdot \left(\frac{t_{FC}}{v_p}\right)^2 \cdot \left(\frac{\sigma_{Y,FC}}{70}\right), \quad (1)$$

by replacing standoff distance \bar{S} in it by either the product of twice the honeycomb cell size (A_{cell}) or by the core depth (t_{HC}), whichever is less: $\bar{S} = \min(2 \cdot A_{cell}, t_{HC})$. Here ρ_p and ρ_b are the projectile and front facesheet ("bumper") densities in g/cm³; t_{FC} – thickness of the rear facesheet in mm; v_p – projectile speed in km/s; $\sigma_{Y,FC}$ – facesheet yield strength in ksi. This approach, however, is considered to be a "rough estimate" [5] and does not include other influential parameters, such as foil thickness and material of the core.



In this study, two distinct methods were used to construct honeycomb core parameters sensitive predictive models: a conventional approach based on the development of HCSP-specific ballistic limit equation (BLE), and an approach based on the development and training of an artificial neural network (ANN). The developed predictive models are focused on the most conservative scenario of hypervelocity impact (HVI) at the normal incidence and limited to aluminum HCSP.

2 HVI DATABASE

Implementation of both of these methods relied on a database for HVI on HCSP, which was extracted from Carriere and Cherniaev [6] and included 56 entries. Different panel configurations and their respective ballistic limits, derived from this database, are summarized in Table 1. Here ballistic limit is understood as particle size on threshold of the critical damage mode – perforation/no perforation of the rear facesheet in case sandwich panel targets.

Table 1: Ballistic limits of HCSP configurations considered in the development of new BLE and ANN.

Projectile		Facesheets		Honeycomb		Ballistic limit
Speed, km/s	Material	Material	Thickness, mm	Grade*	Depth, mm	D _{cr} , mm
6.80	Al2017-T4	Al6061-T6	0.41	1/8-5052-0.003	12.7	0.90
6.75	Al2017-T4	Al7075-T6	1.60	3/16-5056-0.001	50.0	1.71
7.00	Al2017-T4	Al6061-T6	1.60	1/8-5052-0.001	25.0	1.70
7.00	Al2017-T4	Al6061-T6	1.60	3/16-5052-0.001	25.0	2.50
7.00	Al2017-T4	Al6061-T6	1.60	1/4-5052-0.001	25.0	2.50
7.00	Al2017-T4	Al6061-T6	1.60	1/8-5052-0.003	25.0	1.50
7.00	Al2017-T4	Al6061-T6	1.60	3/16-5052-0.003	25.0	1.90
7.00	Al2017-T4	Al6061-T6	1.60	1/4-5052-0.003	25.0	2.10
7.00	Al2017-T4	Al6061-T6	1.00	1/8-5052-0.001	50.0	1.10
7.00	Al2017-T4	Al6061-T6	1.00	3/16-5052-0.001	50.0	1.30
7.00	Al2017-T4	Al6061-T6	1.00	1/4-5052-0.001	50.0	1.50
7.00	Al2017-T4	Al6061-T6	1.00	1/8-5052-0.003	50.0	1.10
7.00	Al2017-T4	Al6061-T6	1.00	3/16-5052-0.003	50.0	1.10
7.00	Al2017-T4	Al6061-T6	1.00	1/4-5052-0.003	50.0	1.30
7.00	Al2017-T4	Al6061-T6	1.60	1/8-5052-0.001	50.0	1.50
7.00	Al2017-T4	Al6061-T6	1.60	3/16-5052-0.001	50.0	1.90
7.00	Al2017-T4	Al6061-T6	1.60	1/4-5052-0.001	50.0	2.30
7.00	Al2017-T4	Al6061-T6	1.60	1/8-5052-0.003	50.0	1.50
7.00	Al2017-T4	Al6061-T6	1.60	3/16-5052-0.003	50.0	1.70
7.00	Al2017-T4	Al6061-T6	1.60	1/4-5052-0.003	50.0	2.10

* Honeycomb grade: cell size (in.) – honeycomb material – foil thickness (in.). For example, 1/8-5052-0.003 stands for a honeycomb with 3.18 mm (1/8 in.) cells made of Al5052 and having a foil thickness of 0.076 mm (0.003 in.).

3 BALLISTIC LIMIT EQUATION

The new BLE for HVI on HCSP proposed in this study is a modification of the Whipple shield BLE, which does not alter the general expression provided by eqn (1), however the expression for \bar{S} in our BLE was supplemented by additional terms, such that:



$$\bar{S} = K \cdot A_{\text{cell}} \cdot \left(\frac{t_{\text{HC}}}{t_{\text{FC}} + \alpha} \right)^{\beta} \cdot \left(\frac{t_{\text{HC}}}{t_{\text{foil}}} \right)^{\gamma} \cdot \left(\frac{30}{\sigma_{Y,\text{HC}}} \right)^{\delta} \quad (2)$$

Here t_{HC} = honeycomb depth in mm; t_{FC} = thickness of a facesheet in mm; t_{foil} = thickness of the honeycomb foil in mm; $\sigma_{Y,\text{HC}}$ = yield strength of the honeycomb material in ksi (e.g., 30 ksi for Al5052 and 50 ksi for Al5056 honeycomb); and K , α , β , γ , δ are parameters with the values given in Table 2.

Table 2: Parameters of the new HCSP BLE.

BLE parameter	K	α	β	γ	δ
Value	2.63	1.893	-0.804	0.304	1.915

The new BLE fit factors presented in Table 2 were determined by minimizing the discrepancy (expressed in terms of the sum of squared errors) between the BLE predictions and the HVI database data provided in Table 1. The goodness-of-fit diagram for the BLE proposed in this study is shown in Fig. 1.

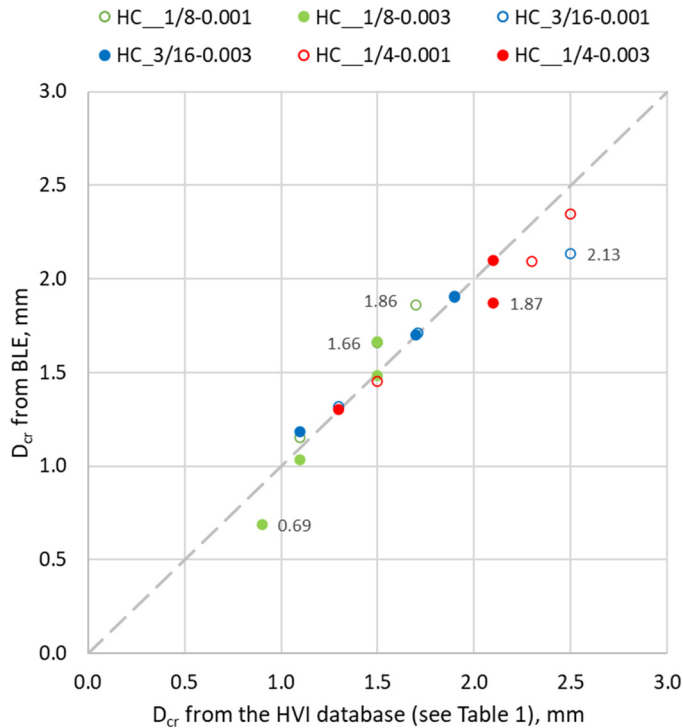


Figure 1: Goodness of fit diagram for the new BLE.

4 ARTIFICIAL NEURAL NETWORK

In this study, MATLAB's Deep Learning Toolbox was used to develop an ANN capable of predicting perforating/non-perforating outcomes of HVI of all-aluminum HCSP structures

and projectiles at normal incidence. A binary output classification scheme was established with the pass “non-perforating” and fail “perforating” classes set. A perforating case is defined as being when the fragments fully penetrate through the rear facesheet.

Input parameters for the ANN included projectile speed and diameter, facesheet material and thickness, honeycomb depth, material, foil thickness and cell size. The developed ANN featured root mean squared propagation activation function, node sizing of 3 and a single hidden layer.

Training sets were established using a hold-out validation scheme, using 80% of the database, for the ANN to learn and develop relations. Once developed, the remaining 20% of the database located in the testing set, were used as “true” prediction scenarios, allowing for analysis of the ANN’s predictive accuracy against known outcomes in the database. The accuracy of ANN predictions was estimated as 85%.

5 VERIFICATION OF BLE AND ANN

Additional datapoints found in Carriere and Cherniaev [6] that have not been used in either BLE fitting or ANN training and, thus, were “unfamiliar” to both, were employed to conduct verification of the developed predictive models. It should be noted that data in Carriere and Cherniaev [6] was obtained by running a detailed numerical model of HVI on HCSP.

Table 3 compares the ballistic limit predictions of the new BLE, ANN and the data from Carriere and Cherniaev [6]. As can be deduced from the table, in all cases, the BLE demonstrated an excellent correlation with the predictions of the sophisticated numerical model, with the discrepancy ranging from 1.13% to 5.58% only. Critical projectile diameter estimations by the ANN closely resembled the simulation ballistic limits: the difference between simulation and ANN predictions ranged between 0.67% and 7.27%.

Table 3: Verification of BLE and ANN predictions.

Projectile		Facesheets		Honeycomb		Ballistic limit		
Speed (km/s)	Material	Material	Thickness (mm)	Grade*	Depth (mm)	D _{cr} (mm)		
						Ref. [6]	BLE	ANN
7.00	Al2017-T4	Al6061-T6	1.30	1/8-5052-0.001	25.0	1.50	1.58	1.53
7.00	Al2017-T4	Al6061-T6	1.60	3/16-5052-0.003	38.0	1.70	1.78	1.76
7.00	Al2017-T4	Al6061-T6	1.00	5/32-5052-0.002	50.0	1.10	1.16	1.18
7.00	Al2017-T4	Al6061-T6	1.30	5/32-5052-0.002	38.0	1.50	1.48	1.51
7.00	Al2017-T4	Al7075-T6	1.00	1/4-5056-0.001	50.0	1.30	1.26	1.26

6 CONCLUSIONS

The new ballistic limit equation is based on the Whipple shield BLE, in which the standoff distance between the facesheets was replaced by a function of the honeycomb cell size, foil thickness, and yield strength of the HC material. The corresponding fit factors were determined by minimizing the sum of squared errors between the BLE predictions and the results of HVI tests listed in the database. The BLE was then tested against a new set of simulation data and demonstrated an excellent predictive accuracy, with the discrepancy ranging from 1.13% to 5.58% only.

The artificial neural network was developed using MATLAB’s Deep Learning Toolbox framework and was trained utilizing the same HCSP HVI database as was employed for the BLE fitting. The developed ANN utilized the root mean square propagation activation function and one hidden layer with three nodes. The ANN demonstrated a very good



predictive accuracy, when tested against a set of simulation data not previously used in the training of the network, with the discrepancy ranging from 0.67% to 7.27%.

ACKNOWLEDGEMENT

This work was financially supported by the Natural Sciences and Engineering Research Council of Canada through Discovery Grant No. RGPIN-2019-03922 “Orbital debris impact survivability models for robotic satellites”.

REFERENCES

- [1] Adams, D.O. et al., Multi-functional sandwich composites for spacecraft applications: An initial assessment. NASA/CR-2007-214880, 2007.
- [2] Bylander, L.A., Carlström, O.H., Christenson, T.S.R. & Olsson, F.G.A., Modular design concept for small satellites. *Smaller Satellites: Bigger Business?*, Springer: Netherlands, pp. 357–358, 2002.
- [3] Cherniaev, A. & Telichev, I., Weight-efficiency of conventional shielding systems in protecting unmanned spacecraft from orbital debris. *Journal of Spacecraft and Rockets*, **54**(1), pp. 75–89, 2016.
- [4] Lathrop, B. & Sennett, R., The effects of hypervelocity impact on honeycomb structures. *9th Structural Dynamics and Materials Conference*, American Institute of Aeronautics and Astronautics, 1968.
- [5] Christiansen, E.L. et al., Handbook for Designing MMOD Protection, NASA JSC-64399, Version A, JSC-17763, 2009.
- [6] Carriere, R. & Cherniaev, A., Honeycomb parameter-sensitive predictive models for ballistic limit of spacecraft sandwich panels subjected to hypervelocity impact at normal incidence. *Journal of Aerospace Engineering*, **35**(4), 2022.
DOI: 10.1061/(ASCE)AS.1943-5525.0001436.

